scientific reports

Check for updates

OPEN

Comparative study of microscale and macroscale technique for encapsulation of *Calotropis gigantea* extract in metal-conjugated nanomatrices for invasive ductal carcinoma

Ayesha Aftab[1], Bashir Ahmad[1]✉, Shazia Bashir[2]✉, Saima Rafique[3], Muhammad Bashir[2], Tayyaba Ghani[4], Asma Gul[1], Atta Ullah Shah[5], Ranjha Khan[6] & Abdulrahim A. Sajini[7,8]

The encapsulation of plant extract in nanomatrices has limitations due to its adhesion to walls, size control, high cost and long durations that results in low yield. Macroscale and microscale level techniques for development of micro/nanoparticles may impact the encapsulation of plant extract. This study aimed to evaluate the relative efficiency of microscale and macroscale techniques for encapsulation of plant extract, which is not compared yet. Keeping this in view, encapsulation of *Calotropis gigantea* leaves extract (CaG) was attained in silver-conjugated poliglusam nanomatrices (POL/Ag) to induce apoptosis in invasive ductal carcinoma (IDC) cells. The ethanolic CaG extract was prepared using percolation method and characterized by chemical tests for its active phytochemical compounds. The droplet-based microfluidic system was utilized as microscale encapsulation technique for CaG in nanomatrices at two different aqueous to oil flow rate ratios 1.0:1.5, and 1.0:3.0. Moreover, conventional batch system was utilized as macroscale encapsulation technique consisted of hot plate magnetic stirrer. The prepared nanomatrices were analysed for antioxidant activity using DPPH test and for cytotoxicity analysis using MCF-7 cells. The characteristic peaks of UV–Vis, FTIR and XRD spectrum confirmed the synthesis of CaG(POL/Ag) by both the encapsulation methods. However, microfluidic system was found to be more expedient because of attaining small and uniform sized silver nanoparticles (92 ± 19 nm) at high flow rate and achieving high encapsulation efficiency (80.25%) as compared to the conventional batch method (52.5%). CaG(POL/Ag) nanomatrices found to have significant antioxidant activity ($p = 0.0014$) against DPPH radical scavenging activity. The CaG(POL/Ag) of the smallest sized formulated by the microfluidic system has also shown the highest cytotoxicity (90%) as compared to batch method (70%) at 80 µg/mL. Our results indicate that the microscale technique using microfluidic system is a more efficient method to formulate size-controlled CaG(POL/Ag) nanomatrices and achieve high encapsulation of plant extract. Additionally, CaG(Pol/Ag) was found to be an efficient new combination for inducing potent ($p < 0.0001$) apoptosis in IDC cells. Therefore, CaG(Pol/Ag) can be further tested as an anti-cancer agent for in-vivo experiments.

[1]Department of Biological Sciences, International Islamic University, H10 Campus, Islamabad, Pakistan. [2]Department of Physics and Applied Mathematics, Pakistan Institute of Engineering and Applied Sciences, Islamabad, Pakistan. [3]Department of Physics, Air University, Islamabad, Pakistan. [4]Department of Metallurgy and Material Engineering, PIEAS, Islamabad 45650, Pakistan. [5]National Institute of Laser and Optronics (NILOP), Islamabad 44000, Pakistan. [6]UCSF/Benioff Children's Hospital, San Francisco, CA, USA. [7]Department of Biomedical Engineering, Khalifa University of Science and Technology, Abu Dhabi 127788, United Arab Emirates. [8]Healthcare Engineering Innovation Center (HEIC), Department of Biomedical Engineering, Khalifa University, Abu Dhabi 127788, United Arab Emirates. ✉email: bashir.ahmad@iiu.edu.pk; shazia@pieas.edu.pk

Nanoparticles have been studied extensively in cancer research because of their unique characteristics which facilitates scientists in diagnostic and treatment of cancer[1]. These particles can be formulated in distinctive ways to control particle size to not only act as anti-cancer agents but also serve as delivery vector for drug. As compared to conventional drugs, nanodrugs emerges as more significant improving stability, biocompatibility, biodegradability, crossing blood–brain barriers and especially providing a valuable targeted therapy[1,2]. In cancer treatment nano drug delivery is providing a more promising efficacy because they can be formulated to provide a shell (e.g. liposome), capsules (oil/water or polymeric membrane), embedding matrix like nanomatrices (polymeric) or pH-temperature sensitive drug-conjugation[3]. The conjugation of polymer embedding metallic nanoparticles is a hybrid combination and may provide an embedding and conjugation system to achieve high-definition encapsulation of any anti-cancer agent[3,4].

Invasive ductal carcinoma (IDC) is one of the most common globally occurring and lethal type of breast cancer[5]. The recent research is focused to prevent and treat this cancer at early stages[6,7]. However, the synthetic chemo-drugs available in the market but comes with severe side effects. Medicinal plants are source of natural products with various biological activities like antiviral, hypoglycaemic, antibiotic, antioxidant, anticancer, antifungal, anti-hypertensive, and insecticide[8]. *Calotropis gigantea* (*C. gigantea*) is one of the abundantly occurring medicinal plant that usually found in northern areas of Pakistan[9,10], and is comprised of many bioactive components including phenols, flavonoids, alkaloids etc.[11,12]. The rich source of phytochemicals makes it possible to use *C. gigantea* against several illness like inflammatory, microbial infection, wound healing,[13] and apoptosis of cancer cells[9,10,14]. Furthermore, the extract of plant like CaG is a mixture of multiple bioactive components and their delivery at cancer site is very difficult in human complex body[15,16]. To overcome the problem of biodistribution and bioavailability of degradable plant extracts the advanced research has focused on preparation of nano or micromatrices[17]. These encapsulating matrices will not only safely deliver the plant extract but will also enhanced their therapeutic efficacy[18]. The extract of *C. gigantea* (CaG) has not been previously formulated with any nanoparticles for IDC cells and it is reported in this study.

The encapsulation of plant extract in micro/nanoparticles such as polymers, cyclodextrins, solid dispersions and liposomes has emerged to be a most competent encapsulating agents[18]. Poliglusam is extensively used as microcarrier/micromatrices for safe delivery of anti-cancer and anti-microbial drugs as well as the plant-based drugs because of its natural biodegradable groups and performance delivery[17,19,20]. The poliglusam micromatrices can also be conjugated to the metals like silver nanoparticles (AgNPs) which will not only aid the encapsulation efficiency of poliglusam but also increase the cytotoxicity of nanoparticles[21]. These arrangements and modifications provide enhance surface interaction with cancer cells and allow extract to combat resistance in complex human body[22–24].

There are several methods, reported previously, for encapsulation of plant extract at micro and macroscale level[25,26]. The encapsulation methods can be divided into two techniques on basis of size of reactor for mixing reagents[26,27]. The microscale level consists of reactor that is 1 to 100 µm in diameter[28,29]. While reactor above 100 µm forms the macroscale level for encapsulation[27]. Microscale techniques may include the microemulsions[30] formed by microfluidic system and phase inversion precipitation[29]. The macroscale techniques may include the spray drying, hot plate magnetic stirring, fluid bed coating, and ion gelation methods of encapsulation[25]. These methods and type of nanoparticles used in encapsulation depends upon the chemical nature of plant extract, i.e. oil based, volatile or high water soluble[16,25]. However, they have many different reported limitations such as extract adhere to the walls in spray drying, takes long duration for encapsulation, high cost due to use of high amount of nanoparticles and size control of encapsulation material[25]. These problems will not only cause denaturation of medicinal plant extract but will also results in low yield of encapsulation in nanomatrices. Microfluidic system is an efficient and precise technique for synthesis of size and shape control nanoparticles including nano/micromatrices. The PMMA microchip-based encapsulation of plant extract has been performed previously with up to 77.125% encapsulation efficiency (EE) of micromatrices[31]. The PMMA microchip was used for water in oil microemulsion in order to synthesize controlled sized nanoparticles and encapsulate the plant extract[31]. These microchips can also be modified for oil in water emulsion system depending upon the nature of plant extract.

To the best of our knowledge, the relative significance of microscale and macroscale techniques for encapsulation of plant extract has not been reported so far. Therefore, this research focuses on studying and comparing the two techniques at microscale and macroscale level for loading plant extract in nanomatrices. For this purpose, the CaG plant extract has been encapsulated in poliglusam-silver (Pol/Ag) nanomatrices at macroscale using conventional batch method and microscale using microfluidic system. We hypothesised that microfluidic system is a competent method for encapsulation of plant extract as compared to conventional wet chemical method (conventional batch method). This new combinational nanomatrices were also examined for its antioxidant and anti-proliferative effect against IDC cells.

Material and methods

Material. Poliglusam (low molecular weight, CAS: 9012-76-4, Sigma, gifted from University of Science and Technology of China), silver nitrate ($AgNO_3$, Duksan), ethanol, acetic acid, canola oil (Sigma), sodium hydroxide (NaOH), 2,2-diphenyl-1-picrylhydrazyl (DPPH, Sigma), dimethyl sulfoxide (DMSO), chloroform, sulphuric acid, hydrogen chloride (HCl), Mayer's reagent, ammonia solution and ferric chloride. All mentioned chemicals are of analytical grade.

Plant collection and extract preparation. The plant materials used in this study were collected from wild areas in Islamabad, Zero-point Latitude: 33° 41′ 37.00" N and longitude: 73° 03′ 54.00" E, after identification by the Dr. Mushtaq Ahmad, Director of Botanical Garden & Herbarium of Islamabad, Pakistan and Quaid-i-Azam University Islamabad, Pakistan. The plant specimen was authenticated by comparison with herbarium

specimen of Islamabad Herbarium of Pakistan and submitted with voucher number ISL-769 in this herbarium for future reference. Following the rules of national action plan of the Pakistan, the leaves of plant (*Calotropis gigantea* (L.) W.T. Aiton, http://legacy.tropicos.org/Name/2603210?projectid=32) were cut with clean scissors and brought for further identification by renowned plant taxonomist (Quaid-i-Azam University Islamabad). The research was in compliance with local policies and regulations of Federal region. The plant was washed with distilled water, dried under shade and ethanolic extract was prepared by following the reported percolation method[31] at Pakistan Institute of Engineering and Applied Sciences (PIEAS), Islamabad, Pakistan. The percentage yield of extract was calculated using the following formula.

$$\%yield = \left(\frac{We}{Ws}\right) X100$$

Here, W_e is the weight of dried extract and W_s is the weight of dried CaG leaves sample. The CaG leaves were air dried and weigh, while extract solvent was evaporated using rotatory evaporator (SENCO) at 30 °C and weighed for percentage yield calculation[31].

Preliminary phytochemical screening of CaG extract. The phytochemical analysis of ethanolic CaG extract was accessed by different chemical tests for terpenoids, flavonoids, phenols, and alkaloids by the reported tests[12,32,33]. For terpenoids detection, chloroform was added to plant extract in ratio of 2:5 and then 1 mL of sulphuric acid was added. For alkaloids, equal amount of HCL and extract was added. After mixing the three drops of Mayer's reagent were added. The presence of flavonoids was indicated by the yellow colour when ammonia solution was added followed by few drops of sulphuric acid into the extract in equal ratio. Lastly, for phenols detection the ethanolic extract was diluted with distilled water and three drops of 10% ferric chloride was added[33].

Experimental setups for synthesis and encapsulation. The Pol/Ag was prepared by the conventional batch method and microfluidic systems in order to compare the encapsulation of CaG using the macroscale and microscale techniques, respectively. The experimental setup is illustrated in Fig. 1.

Macroscale encapsulation using conventional batch setup. The experimental setup of conventional batch method consisted of hot plate magnetic stirrer to prepare the CaG loaded poliglusam-silver nanomatrices (CaG-(Pol/Ag)) at macroscale[34] with few modifications as shown in Fig. 1A. The 1.5% of poliglusam (prepared in 2% of acetic acid solution) was subjected to heating and magnetic stirring at 95 °C and 120 rpm, respectively. A 4 mM of $AgNO_3$ solution was added drop wise into poliglusam solution in ratio 2:1 (poliglusam : $AgNO_3$) and left for 2 h of stirring. For encapsulation of CaG, 10 mg/mL of CaG was mixed into the poliglusam solution and $AgNO_3$ was added drop by drop. After collection of nanomatrices the 10% of NaOH was added drop wise in volumetric ratio of 0.1:1; NaOH: $AgNO_3$. These samples were washed three times with deionized water

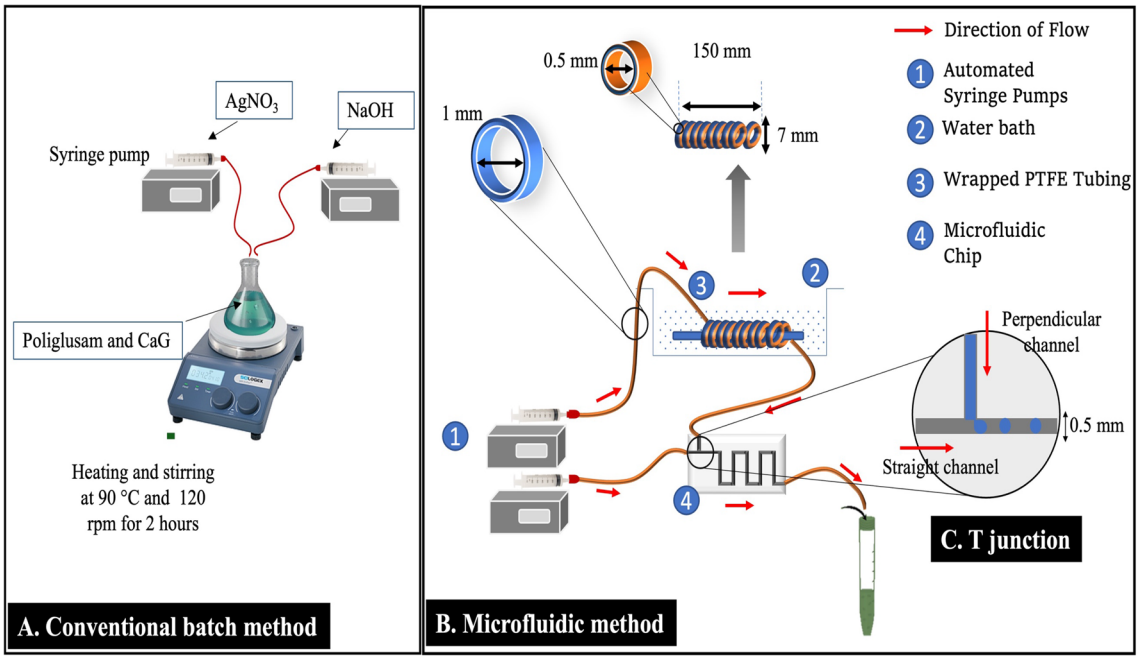

Figure 1. The experimental setup for synthesis of CaG-loaded POL/Ag. (**A**) Conventional batch method using magnetic stirrer. (**B**) Automated microfluidic system consisted of syringe pumps and microchip of 0.5 mm channel. (**C**) T junction and the perpendicular and straight channels for formation of microemulsion in microchip.

($d.H_2O$) by centrifugation at 10,000 rpm for 30 min each time and lyophilized for storage at room temperature and characterization.

Microscale encapsulation using microfluidic system. The microfluidic system was used for synthesis of CaG-(Pol/Ag) at microscale which is shown in Fig. 1B. Two syringe pumps were used for dispensing of precise flow rates which are controlled by automated computer system. The poly-methyl methacrylate (PMMA) microchip developed previously in our lab[35] having T junction was used for the microemulsion formation. The straight channel carries the continuous phase (canola oil) and perpendicular channel carries the dispersed phase (poliglusam, CaG and $AgNO_3$ reaction mixture) shown in Fig. 1C. The dispersed phase contains 1.5% of poliglusam, 4 mM of $AgNO_3$ and 10 mg/mL of CaG. First of all the dispersed phase is passed through the polytetrafluoroethylene (PTFE) microreactor immersed in water bath to heat the solution up to 90 °C[31]. The homogenous and stable microemulsions (water-in-oil) were formed by controlling the flow rates of both the phases. The total flow rate (TFR, mL/h) ratio of aqueous: oil was set as 0.4: 0.6 (F1) and 1.8: 5.4 (F2) and relative flow rate (RFR) ratio of 1:1.5 (F1), and 1:3 (F2). The samples were collected and 10% of NaOH was added to them (0.1:1, NaOH: $AgNO_3$) for acceleration of reduction of $AgNO_3$. The collected samples were washed and stored. In order to compare both methods with equal parameters, the stirring time set for batch system was 2 h which equals to the time taken by microfluidic system to collect equal volume of nanomaterial suspension.

Determination of encapsulation efficiency. The percentage encapsulation efficiency (%EE) of Pol/Ag nanomatrices synthesized by microfluidic system and conventional batch method was calculated by measuring the free drug present in samples. For this, the CaG extract from Pol/Ag nanomaterial was separated using 10,000 rpm centrifugation for 30 min and the amount of free drug in supernatant was calculated using UV–Vis spectrophotometer at 340 nm[31]. The %EE was calculated by following formula.

$$\%EE = \frac{Tp - Fp}{Tp} X100$$

where Tp is total CaG used in encapsulation and Fp is free CaG detached from Pol/Ag.

Characterization of nanomaterial. The physical characteristics, morphology and size of particles were characterized by scanning electron microscope (SEM), X-ray powder diffraction (XRD), Fourier-transform infrared spectroscopy (FTIR), Dynamic light scattering (DLS) and ultraviolet visible (UV–Vis) spectroscopy.

Total antioxidant capacity (TAC). The TAC of CaG and CaG-loaded nanomaterial was evaluated by 1, 1-Diphenyl-2- picrylhydrazyl (DPPH) solution test by using the reported protocol[32]. 0.1 mM of DPPH solution was prepared in ethanol and immediately absorbance was taken at 517 nm for control reading using 96 well plate spectrophotometer (Thermo Fisher scientific). The different concentrations, 40, 60, 80, 100, 120 and 160 µg/mL of ascorbic acid, CaG, and CaG-(Pol/Ag) nanomatrices were prepared in DMSO, and DPPH solution was added in ratio of 1:3; DPPH: antioxidant. The mixtures were shaken vigorously and placed in dark for 30 min at room temperature. The absorbance of each sample was measured at 517 nm. Here, the ascorbic acid was used as standard.

Anti-cancer activity. The CaG-(Pol/Ag) nanomatrices produced from batch and microfluidic methods were tested against the IDC cells (MCF-7) by MTT assay[31]. The 96 well plate was prepared by seeding MCF-7 ($1X10^7$ cells/well) cells and cultured in RPMI media for 24 h at 37 °C. The different formulations of nanomaterial with different concentrations were added into the wells and further incubated for 24 h. Afterwards, the media was removed and MTT dye (5 mg/ mL) was added into each cell, incubated for 2 h and DMSO was added to solubilize the formazan crystals. The absorbance of each cell was taken at 570 nm using the micro-plate reader. the percentage (%) cell viability was calculated using the following formula.

$$\%Cell\ viability = \frac{Abs(sample)}{Abs(control)} X100$$

where, the abs(sample) and abs (control) are the absorbance of sample and control respectively.

Statistical data analysis. The statistical data analysis was performed using GraphPad prism v.9. IC50 values were calculated and Dunnett's multiple comparisons test was applied. Two-way ANOVA was also accessed. The threshold values were set as 0.05 and sstatistical significance was established when $^{*}p < 0.05$, $^{**}p < 0.01$, $^{***}p < 0.001$ and $^{****}p < 0.0001$. The nanomaterial and droplet size were measured by ImageJ software. The Mean and standard deviation (SD) were calculated by Graph Pad prism v.9

Results

Plant extract phytochemical analysis. The CaG extract was prepared using the ethanol as solvent by percolation method. The 50 g of dried leaves of CaG has given 9.8 g of ethanolic extract and the yield of 19.6%. This extract was found to be positive for terpenoids, alkaloids, flavonoids and phenols as indicated by reddish-brown layer at interface, orange, yellow and green colour respectively. Those findings are in accordance with previous reported studies[9,10,12] In another research, the ethanolic extract of *C. gigantea* has 46.75 mg of flavonoid and 33.71 mg of phenolic content[14]. The previous reported studies from HPLC and GCMS data also confirms

the presence of several pharmacological antioxidant compounds[36–38] like terpenoids like Lupeol[38], Urs-12-EN-28-Oic acid, oleanolic acid, 3-O-Acetyl-6-Methoxy-Cycloartenol., ketone like; 3.Alpha.-(Trimethylsiloxy) Cholest-5-Ene., sapogenin, natural steroids like; methylcholesta-4,6-Dien-3-One, terpenes like; caryophyllene, farnesene, and several flavonoids[37] and cardenolides[39].

UV–Vis analysis. The UV–Vis spectrophotometry of synthesized nanomaterial was performed to confirm the formation of CaG-(Pol/Ag) nanomatrices. The change in color from clear to reddish brown indicated the formation of Pol/Ag nanomatrices as shown in Fig. 2B[31,35]. The UV–Vis characteristic peaks of Pol/Ag nanomatrices synthesized by conventional batch method (Ba-CaG(Pol/Ag)) and microfluidic system (Mi-CaG(Pol/Ag)) are shown in Fig. 2A, where an absorbance is visible near 400 nm because of surface plasmon resonance (SPR)

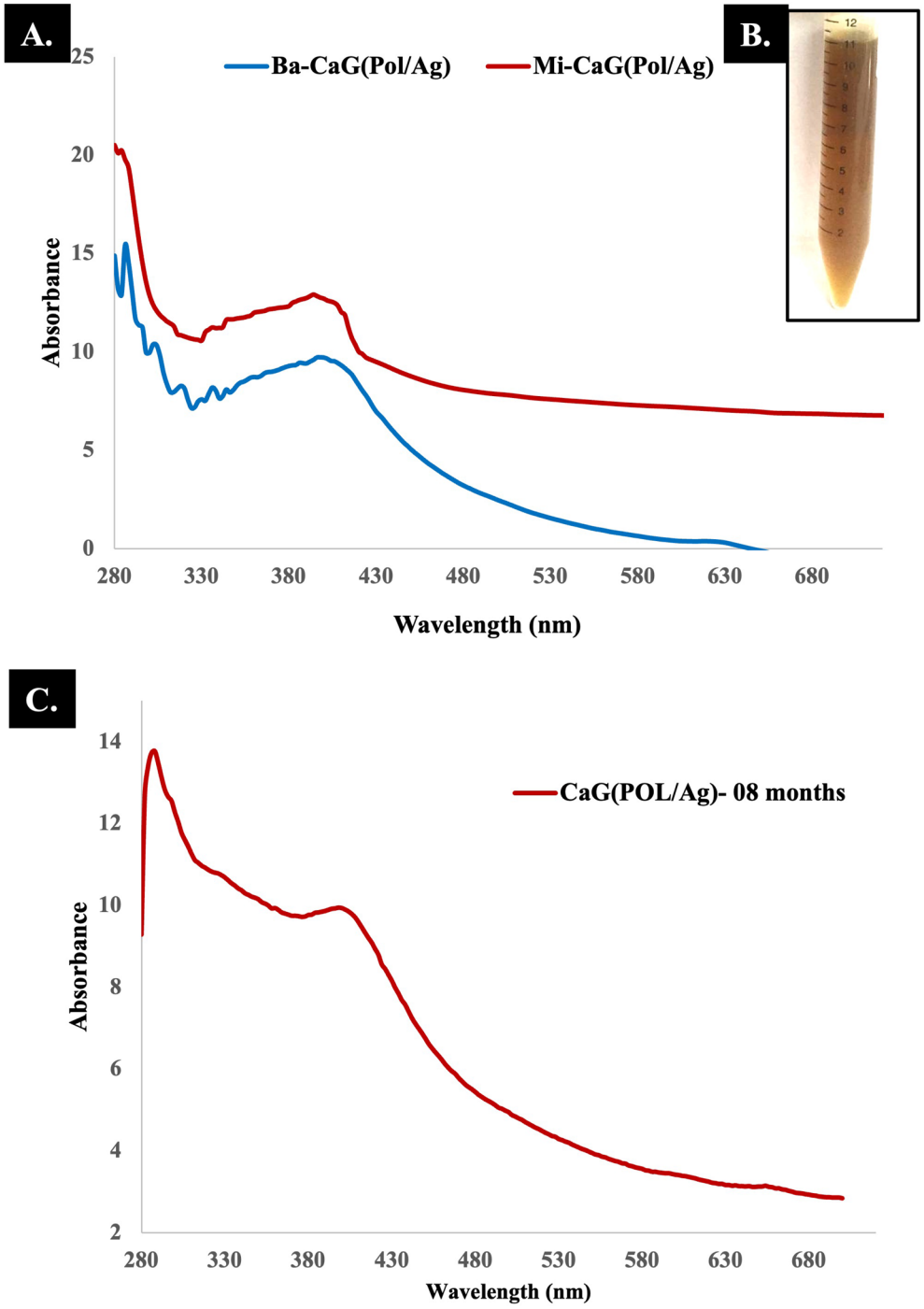

Figure 2. (**A**) The UV–Vis spectra of Ba-CaG(Pol/Ag) and Mi-CaG(Pol/Ag) nanomatrices synthesized by batch and microfluidic system, respectively. (**B**) The suspension of Pol/Ag nanomaterial. (**C**) The UV–Vis spectra of Mi-CaG(Pol/Ag) for eight months stability analysis.

of silver nanoparticles[40]. The silver nanoparticles synthesized by microfluidic system has relatively more absorbance with narrow UV–Vis spectrum, which justify the narrow size distribution of nanoparticles synthesized by microfluidic system. The CaG has peak at 340 nm which is representing the effective encapsulation of CaG in nanomaterial. Furthermore, the peak around 280 nm shows the presence of poliglusam[20]. Altogether these peaks verify the formation of nanomaterial consisted of CaG loaded in poliglusam and silver nanoparticles[31]. The UV–vis spectrophotometry of CaG(Pol/Ag) prepared via the microfluidic system was performed after eight months to check the stability of the nanomatrices. A peak around 400 nm was observed which confirms the presence and stability of AgNPs as shown in Fig. 2C.

% EE of composites. The nanomatrices synthesized by microfluidic system were found to have % EE of 80.25%, while batch system has 52.5%. This shows that microfluidic system is relatively a more competent method to successfully encapsulate the high percentage of CaG extract in nanomaterial. This might be because of rapid mixing in microemulsions in the microfluidic chip[31,35,41]. Recently, Aftab et al., has achieved the 77.125 ± 6.9% EE of *Calotropis procera* in chitosan silver nanoparticles using the microfluidic system[31], while we have not found any other similar study. However, other encapsulation techniques of micro and macro encapsulation has also been reported with many limitations[16,25] as discussed in Sect. 1.

FTIR spectrum. The absorbance of IR by various functional groups of poliglusam, CaG and Pol/Ag prepared by both methods is shown in Fig. 3. It can be noted that CaG(Pol/Ag) has been successfully prepared by both methods. The shifting of pure poliglusam peaks in Pol/Ag nanomatrices may be because of formation of nanomatrices[31,42]. The broadening and elevation of peak around 3280 cm^{-1} shown in Fig. 3A,B as compared to Fig. 3C, and disappearance of poliglusam peak at 1639.78 cm^{-1} is indicating the role of hydroxyl and amino groups in stabilization of silver ions[23,34]. The CaG has displayed (Fig. 3D) the absorption peaks at various intensity which represents the presence of different functional groups existing in it. The absorbance at 1304 cm^{-1}, 1277 cm^{-1} and 1085 cm^{-1} confirming the presence of primary and secondary alcohols, flavonoids, and tertiary alcohol, respectively[43]. These peaks justify the bioactive compounds detected in a forementioned qualitative phytochemical analysis, which plays an important role as antioxidants.

XRD analysis. The 2 θ values of Pol/Ag and CaG analysed by XRD are shown in Fig. 4. The XRD of pure poliglusam (Fig. 4D) has broad peak around 2θ = 20°, which shows the amorphous nature of poliglusam[42]. The

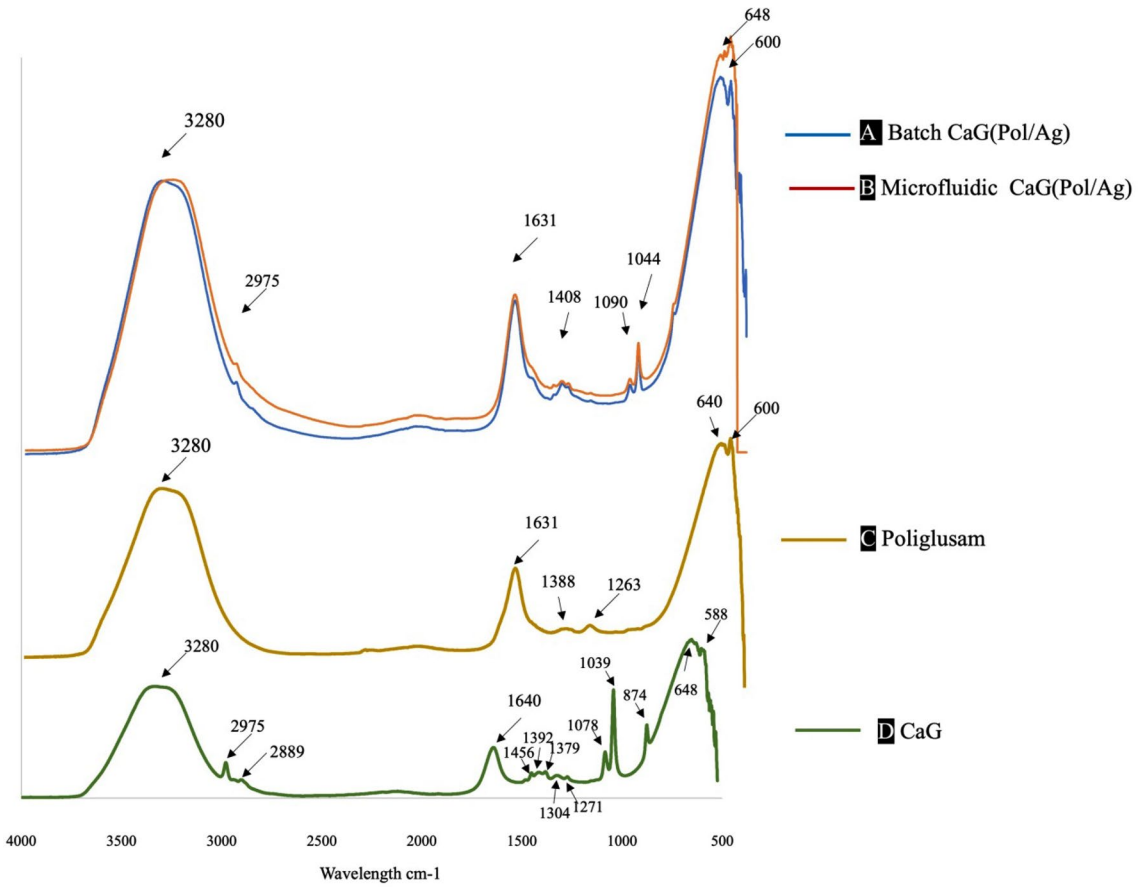

Figure 3. The FTIR of (**A**) Pol/Ag nanomatrices synthesized by conventional batch method and (**B**) microfluidic system, (**C**) poliglusam, and (**D**) *Calotropis gigantea* (CaG).

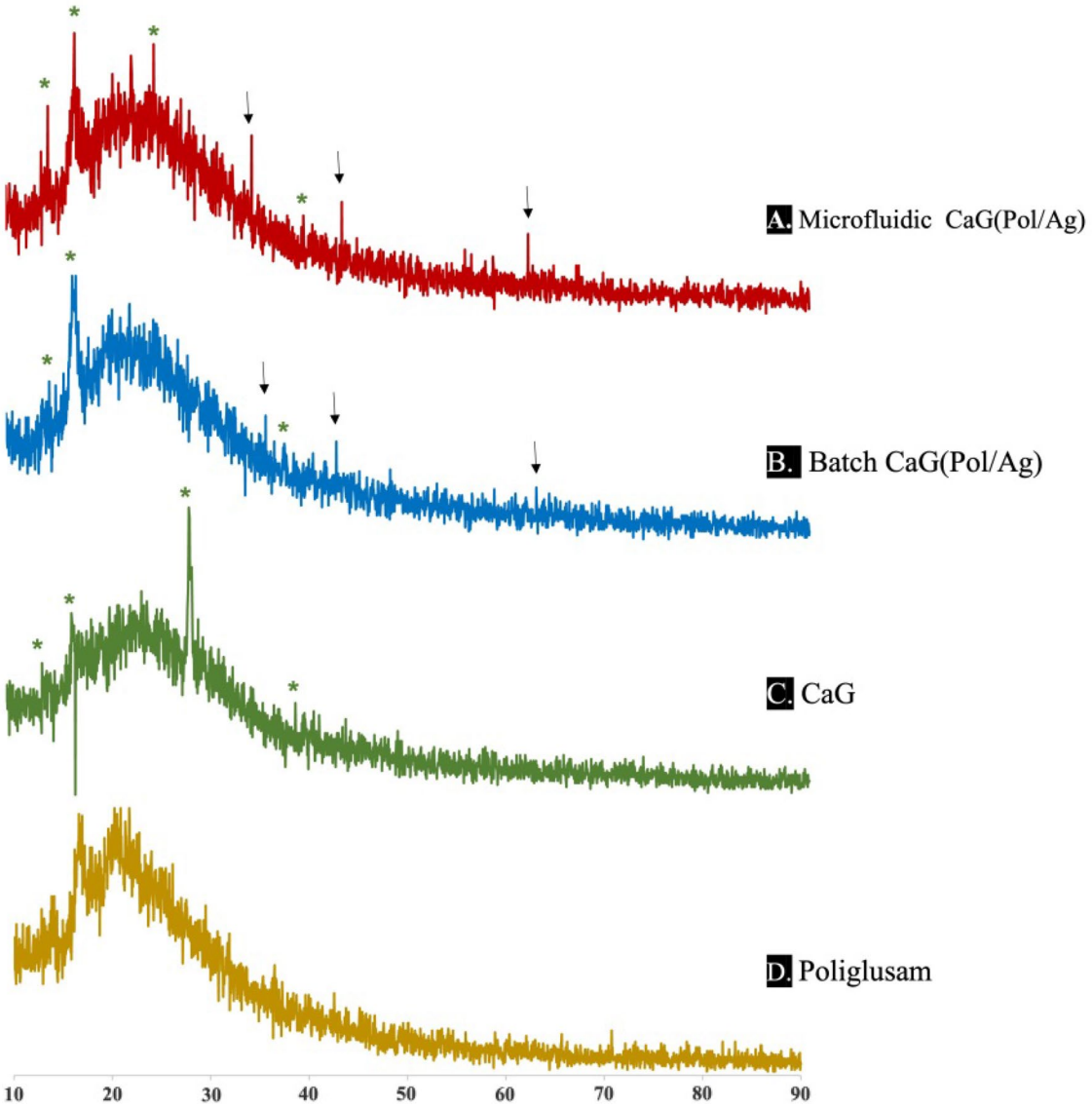

Figure 4. XRD results of CaG(POL/Ag) nanomatrices synthesize through (**A**) microfluidic and (**B**) batch method. (**C**) XRD of CaG extract and (**D**) Poliglusam solution. Arrows indicating characteristic peaks of silver nanoparticles. Asterisks * representing the various peaks of CaG extract.

POL/Ag prepared by microfluidic system and batch method has broad peak around 20°, along with other peaks which indicates the presence of poliglusam and natural product. For microfluidic system the appearance of Brag reflections at 2 $\theta = 34.48°$, 43.44° and 62° and for batch method at $2\theta = 35.84°$, 42.88° and 62.8° are clearly indicating the synthesis of silver nanoparticles[42,44]. The nanomatrices (Fig. 4C,D) have a small diffraction as compared to free natural product (Fig. 4B), which is showing the crystalline form of natural product present in the composites[45].

SEM analysis for size and structural morphology. The microfluidic system was utilised to tune the nanomatrices size at two different flow rates i.e. F1 and F2 as shown in Fig. 5. The SEM was performed to visualise the nanomatrices for size and morphology shown in Fig. 6A–H.

Size analysis. It can be noticed that with the increase in flow rates (TFR and RFR) the size of microemulsion as well the size of silver nanoparticles declined. This is because with the decrease in size of microemulsion the number of nuclei decreases that are formed within each microemulsion which result in decrease in average final size of the nanomaterial[46,47]. The size of microemulsions at two different flow rates in 0.5 mm microchannel was also calculated and has been displayed in Fig. 5. At high flow rate F2, the CaG(Pol/Ag) nanomatrices of size 92 ± 19 nm were formed, while the size of nanomatrices was larger (198 ± 38 nm) at slow RFR (F1). We have also observed a narrow size distribution of nanomatrices with the increase in flow rate. All these finding is in

Flowrate labels	Relative flow rates		Droplet size (mm)	Nanocomposite size	
	Aqueous : oil			Diameter (nm)	Size distribution
F1	1	1.5	0.72	198	36
F2	1	3.0	0.42	92	19

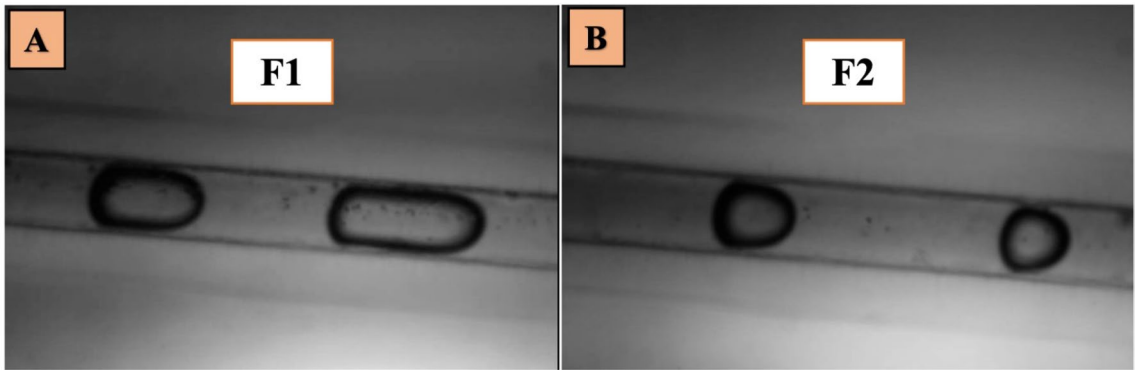

Figure 5. Effect of two different flow rates on droplets and nanomaterial size/size distribution shown in table above. The microchannel and droplets with (**A**) F1 flow rate, and (**B**) F2 flow rate.

consistent with the previous reports[46–49]. Furthermore, the Pol/Ag nanomatrices prepared by the batch method are relatively large in size and are not evenly distributed (Fig. 6A,B).

Morphology analysis. The change in morphology of the nanomaterial captured by SEM was also observed. The SEM images has also shown the bright silver nanoparticles embedded on membrane-type- poliglusam collected from microfluidic system[42]. At high flow rate, the Pol/Ag nanomatrices are more spherical and uniform. On the other hand, the Pol/Ag nanomatrices prepared via a batch method are more irregular in shape/surface. The irregular surface of poliglusam is also not displaying the silver nanoparticles clearly.

Stability analysis. The SEM image was taken after eight months to check the stability of nonmaterices. As shown in Fig. 6G,H, after eight months the size of CaG(Pol/Ag) at flow rate F2 recorded was 119 ± 21 nm. The 27 nm increase in size was recorded which is quite negligible and also the CaG(Pol/Ag) were found to be evenly distributed. These results suggest the stability of nanomatrices.

Overall, these finding shows that microfluidic system plays an important in homogenous mixing for synthesis of narrow size distribution and smooth surface of poliglusam microcarriers. These results also indicate that the size and morphology of nanomaterial can be tuned by microfluidic system.[47,49]. Yanar et al. has produced the size control liposomes[48]. While in this research we have formulated the size controlled poliglusam nanomatrices embedding silver nanoparticles conjugated with plant extract, which were not reported earlier.

Hydrodynamic size and zeta potential. The hydrodynamic size and zeta potential of the microfluidic prepared CaG(Pol/Ag) nanomatrices was analysed using the DLS technique show in Fig. 7A–C. The zeta potential of any nanomaterial above + 30 mV is considered as highly stable and strongly cationic[50]. in this study the zeta potential of the nanomatrices was found to be 42.42 mV. Which suggests that they are highly stable and cationic. This strong cationic nature of the CaG(Pol/Ag) nanomatrices increase the endocytosis activity on the surface of negatively charged cancer cells due to electrostatic force (Fig. 7C). Therefore, this can be assumed that these nanomatrices would have ability to induce apoptosis in cancer cells to great extent. These results are consistent with earlier reported studies where the electric potential of the particles has been measured to be positively charged[51]. The average size of the nanomatrices was measured to be 178.5 nm with polydispersity index of 2.97. The size measured by the DLS is quite close to the size measured by the SEM analysis. These results indicate that CaG(Pol/Ag) nanomatrices are evenly distributed with positive charge on their surface which make them an ideal nanoagent to induce cancer cell death.

Antioxidant properties of CaG and nanomatrices. The reported studies have found valuable phytochemical present in CaG including alkaloid, flavonoids, and phenols. Therefore, it can be used as a natural antioxidant[9,10,12]. The percentage inhibition of free radicals by CaG, CaG(POL/Ag) and standard is shown in Fig. 8. The results shows that CaG alone has adequate potential of antioxidant activity. However, when combined with Pol/Ag nanomatrices, the CaG(Pol/Ag) possess a significant antioxidant activity.

Anti- cancer effect. In this study, the IDC cells, MCF-7, were treated with the microchip-formulated (M-CaG(Pol/Ag)) nanomatrices of two different sizes, MF1-CaG(Pol/Ag) of 198 ± 36 nm and MF2-CaG(Pol/Ag) of 92 ± 19 nm, and batch method synthesized (Ba-CaG(Pol/Ag)) nanomatrices (213 ± 73 nm). Their

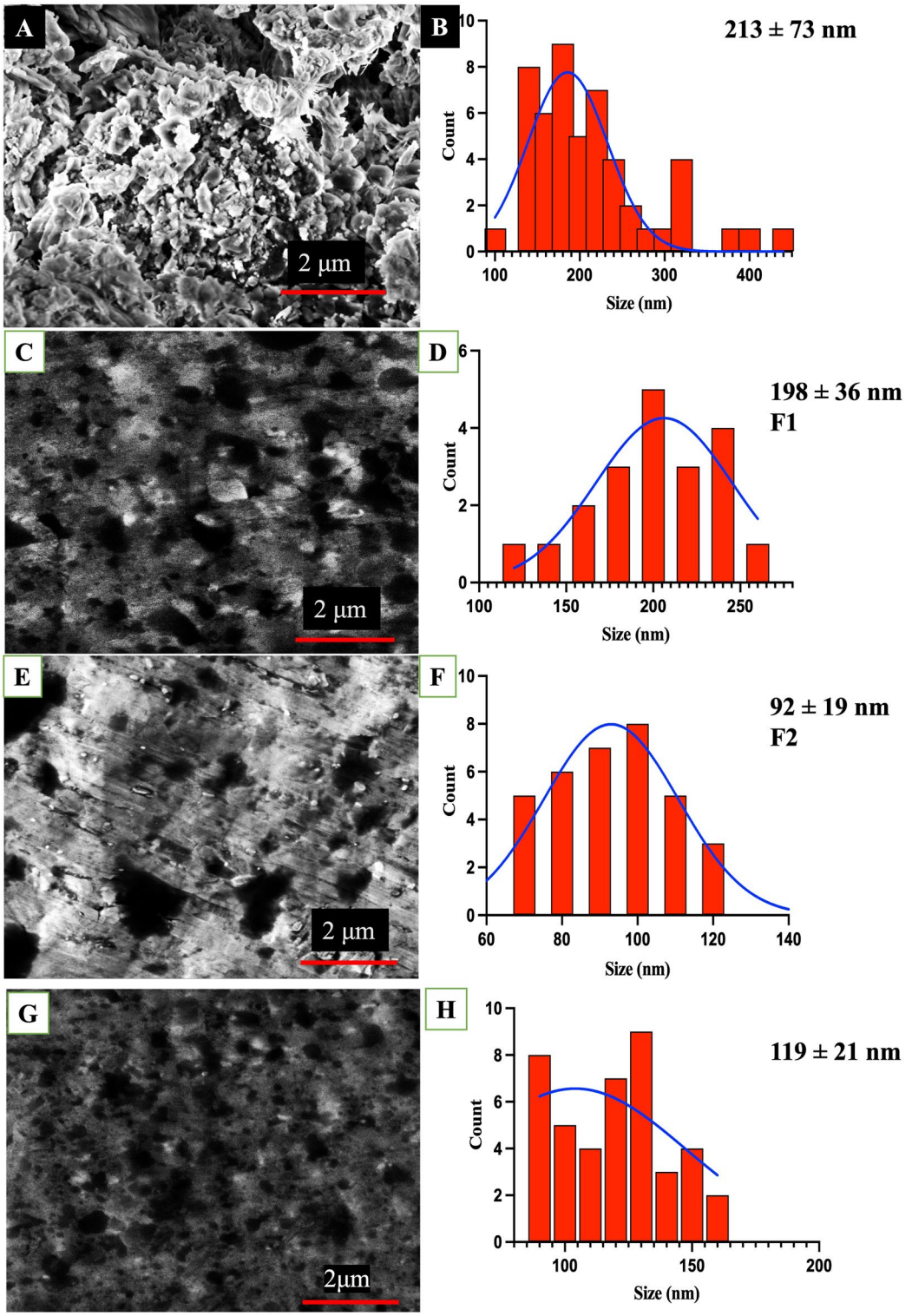

Figure 6. SEM images of CaG(Pol/Ag) nanomatrices. CaG(Pol/Ag) synthesized by batch method is shown in image (**A**) and histogram in (**B**) Synthesised by microfluidic system at different flow rates are shown in images (**C**) and (**E**) and their respective histograms in (**D**) and (**F**). Here flow rate (mL/h) in ratio of aqueous: oil phase is RFR that is F1 = 1:1.5, and F2 = 1: 3. G and H is the SEM image of F2 CaG(Pol/Ag) eight months aged.

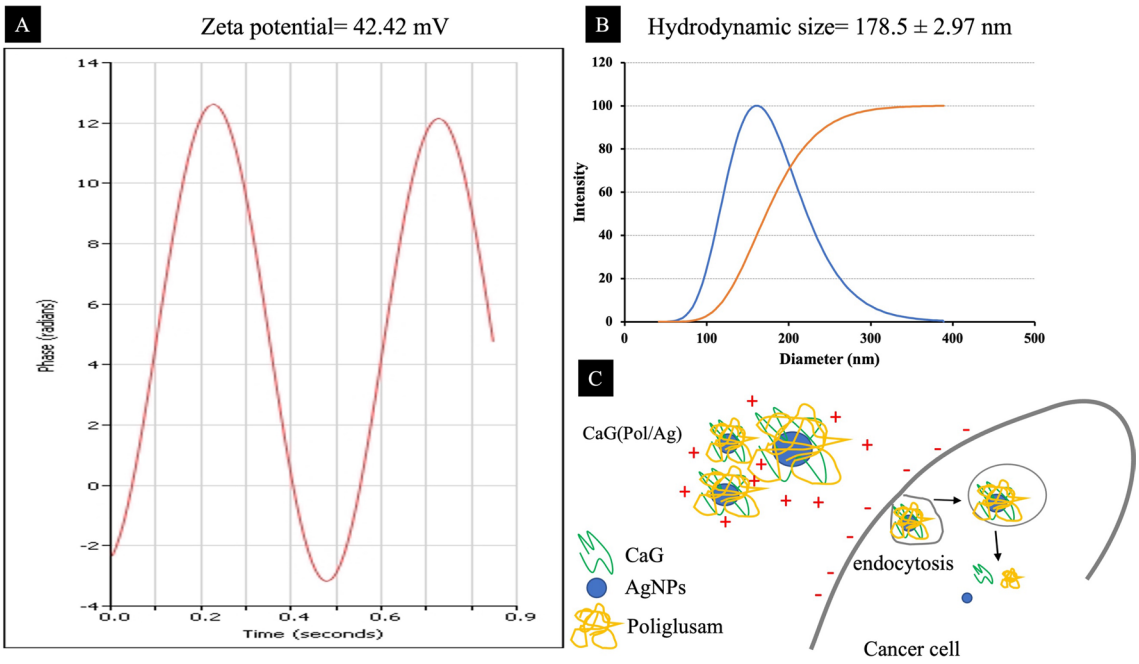

Figure 7. The DLS analysis. (**A**) Zeta potential of CaG(Pol/Ag) nanomatrices. (**B**) Hydrodynamic size calculated via cumulative intensity distribution. (**C**) The diagrammatic representation of electrostatic interaction between CaG(Pol/Ag) nanomatrices and cancer cells aiding the endocytosis.

cytotoxic effect and IC_{50} values are shown in Fig. 9A,B respectively. The CaG(Pol/Ag) nanomatrices synthesised by two different methods has shown quite significant ($p < 0.0001$) anti-cancer activity in increase concentration dependant manner. However, M-CaG(Pol/Ag) nanomatrices has shown more decrease in IDC cells viability as compared to Ba-CaG(Pol/Ag) nanomatrices. At 60 and 80 µg/mL of dose a difference of 30% and 20% of cell viability can be noticed in Fig. 9 by MF2-CaG(Pol/Ag).

Furthermore, we have also found that smallest size particles 92 ± 19 nm (MF2-CaG(Pol/Ag) at 80 µg/mL has the minimum cell viability of 10% (% cytotoxicity = 90). While Ba-CaG(Pol/Ag) nanomatrices has lowest cell viability of 30% (% cytotoxicity = 70) at 80 µg/mL. These results indicate that with the change in size and morphology of nanoparticles, the cell viability of the cancer cells is also affecting. A small size and uniform morphology of Pol/Ag nanomaterial has more potent anticancer efficacy[52–54]. However, in previous studies scientist has also preferred the 50 nm size over 10 or 20 nm[55,56], this may be because the smallest particles may escape the cancer cells easily even before performing their average activity. While, in our study, the size of particle is around 92 nm, which is quite optimal to enter and escape the cancer cells upon their average activity[55].

It can also be observed in this study that the antioxidant-CaG extract has shown 24% cell viability at 80 µg/mL, however conjugating it with tuned size and morphology Pol/Ag nanomaterial has increased the anti-tumour activity[31]. The two-way ANOVA test has confirmed those finding to be statistically significant, $p < 0.0001$.

Conclusion

The present study reports that encapsulation of plant extract at microscale using microfluidic system is more efficient to set out high yield encapsulation efficiency as compared to encapsulation at macroscale using conventional batch method. Also, the microfluidic system provides the flexibility to control the size, shape, and polydispersity of nanomaterial by changing the flow rates of the agents. This research reports the CaG(Pol/Ag) as a new nanotherapeutic agent which is competent to induce apoptosis in MCF-2 cells.

A.

Dunnett's multiple comparisons test	Summary	*p*-Value	Significant?
Ascorbic acid vs. CaG	****	<0.0001	Yes
Ascorbic acid vs. CaG(Pol/Ag)	**	0.0014	Yes

B.

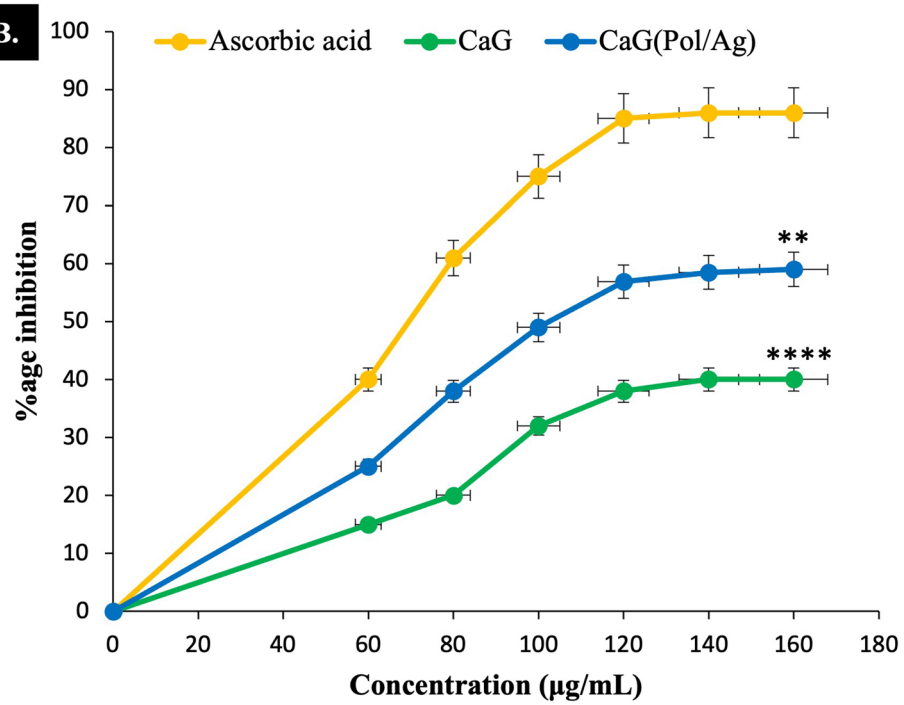

Figure 8. Antioxidant analysis. (**A**) The table statistically demonstrate the significance of CaG(Pol/Ag) by Dunnett's multiple tests. (**B**).The % inhibition graph of ascorbic acid, calotropis gigantea (CaG) and CaG loaded poliglusam-silver nanomatrices (CaG(Pol/Ag)). Here, n = 3 and $^{**}p < 0.01$ and $^{****}p < 0.0001$.

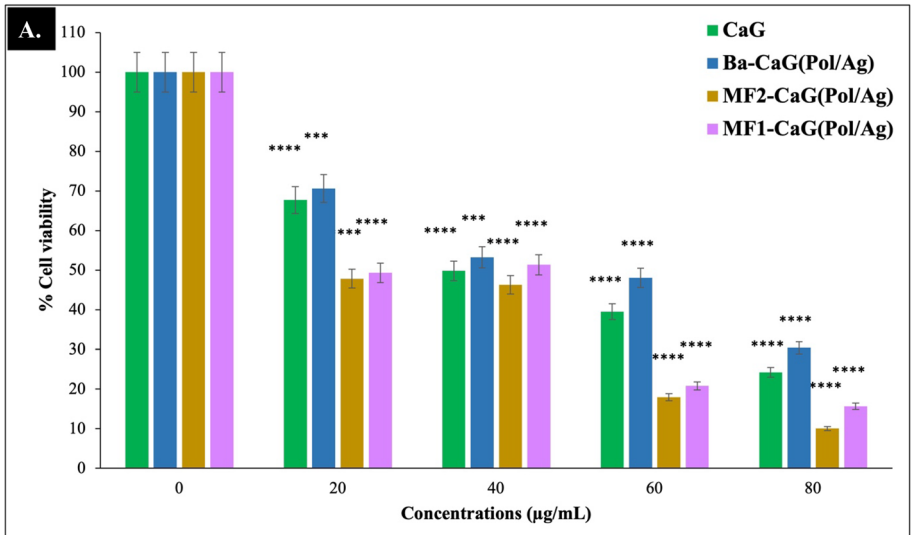

B.

Samples	CaG	Ba-CaG(Pol/Ag)	MF2-CaG(Pol/Ag)	MF1-CaG(Pol/Ag)
IC_{50} (µg/mL)	238±1	50.2±1	48.8±1	48.7±1

Figure 9. (**A**) The % cell viability of CaG extract and CaG-Pol/Ag nanomatrices synthesised by batch method (Ba-CaG(Pol/Ag)) and microfluidic system method, MF1-CaG(Pol/Ag) of 198 ± 36 nm and MF2-CaG(Pol/Ag) of 92 ± 19 nm. (**B**) The IC50 values of each agent against MCF cells.

Data availability

All data generated or analyzed during this study are included in this published article. The Plant *c. gigantea* was collected by following the rules of national action plan of the Pakistan and was dully verified and permitted by Herbarium of Pakistan (Islamabad) Quaid i Azam university Islamabad, Pakistan and identified by renowned plant taxonomist of Islamabad (*Calotropis gigantea* (L.) W.T. Aiton, http://legacy.tropicos.org/Name/2603210?projectid=32.

Received: 30 January 2023; Accepted: 24 July 2023
Published online: 18 August 2023

References

1. Ion, D. *et al.* An up-to-date review of natural nanoparticles for cancer management. *Pharmaceutics* **14**, 18 (2022).
2. Zhu, R. *et al.* Current progress in cancer treatment using nanomaterials. *Front Oncol.* **12**, 3407 (2022).
3. Singh, R. & Lillard, J. W. Nanoparticle-based targeted drug delivery. *Exp. Mol. Pathol.* https://doi.org/10.1016/j.yexmp.2008.12.004 (2009).
4. Nitta, S. K. & Numata, K. Biopolymer-based nanoparticles for drug/gene delivery and tissue engineering. *Int. J. Mol. Sci.* https://doi.org/10.3390/ijms14011629 (2013).
5. Sharma, G. N., Dave, R., Sanadya, J., Sharma, P. & Sharma, K. K. Various types and management of breast cancer: An overview. *J. Adv. Pharm. Technol. Res.* **1**, 126 (2010).
6. Takada, K. *et al.* Factors predictive of invasive ductal carcinoma in cases preoperatively diagnosed as ductal carcinoma in situ. *BMC Cancer* **20**, 1–9 (2020).
7. Zangouri, V. *et al.* Medullary breast carcinoma and invasive ductal carcinoma: A review study. *Iran J Med Sci* **43**, 371 (2018).
8. Armendáriz-Barragán, B. *et al.* Plant extracts: From encapsulation to application. *Expert Opin. Drug Deliv.* **13**, 1165–1175 (2016).
9. Sawong, S. *et al. Calotropis gigantea* stem bark extracts inhibit liver cancer induced by diethylnitrosamine. *Sci. Rep.* **12**, 1–30 (2022).
10. Raji, R. *et al. Calotropis gigantea* fiber—A biogenic reinforcement material for europium substituted hydroxyapatite/poly(3,4-propylenedioxythiophene) matrix: A novel ternary composite for biomedical applications. *ACS Omega* **7**, 6024 (2022).
11. Rani, R., Sharma, D., Chaturvedi, M. & Yadav, J. P. Phytochemical analysis, antibacterial and antioxidant activity of *Calotropis procera* and *Calotropis gigantea*. *Nat. Prod. J.* **9**, 47–60 (2018).
12. Radhakrishnan, S., Alarfaj, A. A. & Annadurai, G. Estimation of phytochemical analysis and invitro antioxidant activity of *Calotropis gigantea* extract: Wound healing activity and its biomedical application. *Int. J. Pharm. Sci. Res.* **6**, 3053 (2015).
13. Altun, İ & Sonkaya, A. The most common side effects experienced by patients were receiving first cycle of chemotherapy. *Iran. J. Public Health* **47**, 1219 (2018).
14. Alafnan, A. *et al.* Evaluation of the phytochemical, antioxidant, enzyme inhibition, and wound healing potential of *Calotropis gigantea* (L.) dryand: A source of a bioactive medicinal product. *Front. Pharmacol.* **12**, 1622 (2021).
15. Soliman, T. N. *et al.* Microencapsulation of plant phenolic extracts using complex coacervation incorporated in ultrafiltered cheese against AlCl3-induced neuroinflammation in rats. *Front. Nutr.* **9**, 1355 (2022).
16. Bilia, A. R. *et al.* Plants extracts loaded in nanocarriers: An emergent formulating approach. *Nat. Prod. Commun.* **13**, 1157–1160 (2018).
17. Kim, J. *et al.* Charged nanomatrices as efficient platforms for modulating cell adhesion and shape. *Tissue Eng. Part C Methods* **18**, 913–923 (2012).

18. Conte, R. *et al.* Polyphenols nanoencapsulation for therapeutic applications. *J. Biomol. Res. Ther.* **5**, 2 (2016).
19. Hussain, S. A., Abdelkader, H., Abdullah, N. & Kmaruddin, S. Review on micro-encapsulation with Chitosan for pharmaceuticals applications. *MOJ Curr. Res. Rev.* **1**, 77–84 (2018).
20. Soleimani, N., Vaseghi, A. & Loconte, V. Poliglusam Nanoparticles activate T cell response in breast cancer cell: An in vivo and in vitro study. *J. Fluoresc* **29**, 1057–1064 (2019).
21. Prusty, K. & Swain, S. K. Nano silver decorated polyacrylamide/dextran nanohydrogels hybrid composites for drug delivery applications. *Mater. Sci. Eng. C* **85**, 130–141 (2018).
22. Bilal, M. *et al.* Biogenic nanoparticle-chitosan conjugates with antimicrobial, antibiofilm, and anticancer potentialities: Development and characterization. *Int. J. Environ. Res. Public Health* **16**, 598–612 (2019).
23. Nate, Z., Moloto, M. J., Mubiayi, P. K. & Sibiya, P. N. Green synthesis of chitosan capped silver nanoparticles and their antimicrobial activity. *MRS Adv.* **3**, 2505–2517 (2018).
24. Kalaivani, R. *et al.* Synthesis of chitosan mediated silver nanoparticles (Ag NPs) for potential antimicrobial applications. *Front. Lab. Med.* **2**, 30–35 (2018).
25. Mudrić, J., Ibrić, S. & Đuriš, J. Microencapsulation methods for plants biologically active compounds: A review. *Lekovite sirovine* **38**, 62–67 (2018).
26. Ahadian, S. *et al.* Micro and nanoscale technologies in oral drug delivery. *Adv. Drug Deliv. Rev.* **157**, 62 (2020).
27. Misra, A., Singh, V. & Parthasarathy, R. Material-tissue interfacial phenomena: Challenges in mathematical modeling. In *Material-Tissue Interfacial Phenomena: Contributions from Dental and Craniofacial Reconstructions* (eds. Spencer, Paulette. & Misra, Anil.) 253–264 (Woodhead Publishing, 2017). https://doi.org/10.1016/B978-0-08-100330-5.00010-8.
28. Focus Microscale reactors: nanoscale products. *Lab Chip* **4**, 11N-15N (2004)
29. Ran, J. *et al.* Microreactor-based micro/nanomaterials: Fabrication, advances, and outlook. *Mater Horiz* https://doi.org/10.1039/D3MH00329A (2023).
30. Jenjob, R., Phakkeeree, T., Seidi, F., Theerasilp, M. & Crespy, D. Emulsion techniques for the production of pharmacological nanoparticles. *Macromol. Biosci.* **19**, 1–13 (2019).
31. Aftab, A. *et al.* Microfluidic platform for encapsulation of plant extract in chitosan microcarriers embedding silver nanoparticles for breast cancer cells. *Appl. Nanosci. (Switzerland)* https://doi.org/10.1007/s13204-020-01433-8 (2020).
32. Truong, D. H. *et al.* Evaluation of the use of different solvents for phytochemical constituents, antioxidants, and in vitro anti-inflammatory activities of severinia buxifolia. *J. Food Qual.* **2019**, (2019).
33. Gul, R., Jan, S. U., Faridullah, S., Sherani, S. & Jahan, N. Preliminary phytochemical screening, quantitative analysis of alkaloids, and antioxidant activity of crude plant extracts from ephedra intermedia indigenous to Balochistan. *Sci. World J.* **2017**, (2017).
34. Chen, Q., Jiang, H., Ye, H., Li, J. & Huang, J. Preparation, antibacterial, and antioxidant activities of silver/chitosan composites. *J. Carbohydr. Chem.* **33**, 298–312 (2014).
35. Bashir, S. *et al.* Droplet-based microfluidic synthesis of silver nanoparticles stabilized by PVA and PVP: Applications in anticancer and antimicrobial activities. *Chem. Pap.* **2022**, 1–12. https://doi.org/10.1007/S11696-022-02403-W (2022).
36. Mutiah, R., Widyawaruyanti, A. & Sukardiman, S. Calotroposid A: A Glycosides Terpenoids from *Calotropis gigantea* induces apoptosis of colon cancer WiDr cells through cell cycle arrest G2/M and Caspase 8 expression. *Asian Pac J. Cancer Prev.* **19**, 1457 (2018).
37. Uthirasamy, S. *et al.* Determining the bioactive constituents in *Calotropis gigantea* leaves by GC-MS, HPLC and FTIR techniques. *New Vis. Biol. Sci.* **1**(1), 1–11 (2021).
38. Loice, R. R., Parthiban, P. & Standly, A. L. The effect of *Calotropis Gigantea* leaf extract on growth control of struvite crystals. *Int. Res. J. Eng. Technol.* **5**, 805–817 (2018).
39. Kharat, K. R. & Kharat, A. S. The *Calotropis gigantea* methanolic extract induces apoptosis in human breast carcinoma cells. *Iran J. Med. Sci.* **44**, 492 (2019).
40. Bankalgi, S. C., Londonkar, R. L., Madire, U. & Tukappa, N. K. A. Biosynthesis, characterization and antibacterial effect of phenolics-coated silver nanoparticles using *Cassia javanica* L. *J Clust Sci* https://doi.org/10.1007/s10876-016-1016-9 (2016).
41. Xu, L., Peng, J., Yan, M., Zhang, D. & Shen, A. Q. Droplet synthesis of silver nanoparticles by a microfluidic device. *Chem. Eng. Process.* **102**, 186–193 (2016).
42. Govindan, S., Nivethaa, E. A. K., Saravanan, R., Narayanan, V. & Stephen, A. Synthesis and characterization of Chitosan-Silver nanocomposite. *Appl. Nanosci. (Switzerland)* https://doi.org/10.1007/s13204-012-0109-5 (2012).
43. Oliveira, R. N. *et al.* FTIR analysis and quantification of phenols and flavonoids of five commercially available plants extracts used in wound healing. *Matéria (Rio de Janeiro)* **21**, 767–779 (2016).
44. Venkatesham, M., Ayodhya, D., Madhusudhan, A., Veera Babu, N. & Veerabhadram, G. A novel green one-step synthesis of silver nanoparticles using chitosan: Catalytic activity and antimicrobial studies. *Appl. Nanosci. (Switzerland)* https://doi.org/10.1007/s13204-012-0180-y (2014).
45. Hussein-Al-Ali, S. H., Kura, A., Hussein, M. Z. & Fakurazi, S. Preparation of chitosan nanoparticles as a drug delivery system for perindopril erbumine. *Polym. Compos.* **39**, 544–552 (2018).
46. Lin, Y. S. *et al.* An Aluminum microfluidic chip fabrication using a convenient micromilling process for fluorescent poly(dl-lactide-co-glycolide) microparticle generation. *Sensors (Basel)* **12**, 1467 (2012).
47. van Ballegooie, C., Man, A., Andreu, I., Gates, B. D. & Yapp, D. Using a microfluidics system to reproducibly synthesize protein nanoparticles: Factors contributing to size, homogeneity, and stability. *Processes* **7**, 1–19 (2019).
48. Yanar, F., Mosayyebi, A., Nastruzzi, C., Carugo, D. & Zhang, X. Continuous-flow production of liposomes with a millireactor under varying fluidic conditions. *Pharmaceutics* **12**, 1–21 (2020).
49. Jahn, A. *et al.* Preparation of nanoparticles by continuous-flow microfluidics. *J. Nanopart. Res.* **10**, 925–934 (2008).
50. Clogston, J. D. & Patri, A. K. Zeta potential measurement. *Methods Mol. Biol.* **697**, 63–70 (2011).
51. Dara, P. K. *et al.* Synthesis and biochemical characterization of silver nanoparticles grafted chitosan (Chi-Ag-NPs): In vitro studies on antioxidant and antibacterial applications. *SN Appl. Sci.* **2**, 1–12 (2020).
52. Pucelik, B. *et al.* Synthesis and characterization of size- and charge-tunable silver nanoparticles for selective anticancer and antibacterial treatment. *ACS Appl. Mater Interfaces* **14**, 14981–14996 (2022).
53. Nam, K. C. *et al.* Particle size dependent photodynamic anticancer activity of hematoporphyrin-conjugated Fe_3O_4 particles. *J Nanomater* **2016** (2016).
54. Albanese, A., Tang, P. S. & Chan, W. C. W. The effect of nanoparticle size, shape, and surface chemistry on biological systems. *Annu. Rev. Biomed. Eng.* **14**, 1–16. https://doi.org/10.1146/annurev-bioeng-071811-150124 (2012).
55. Tang, L. *et al.* Investigating the optimal size of anticancer nanomedicine. *Proc. Natl. Acad. Sci. USA* **111**, 15344–15349 (2014).
56. Bao, H., Zhang, Q., Xu, H. & Yan, Z. Effects of nanoparticle size on antitumor activity of 10-hydroxycamptothecin-conjugated gold nanoparticles: In vitro and in vivo studies. *Int. J. Nanomed.* **2016**, 929–940 (2016).

Acknowledgements

We are thankful to the School of Biological Sciences (SBS), Punjab University, Lahore, Pakistan, for gifting MCF-7 cell lines. We also acknowledge Pakistan Institute of Engineering and Applied Sciences, Islamabad, Pakistan for proving experimental facility and resources for conducting microfluidic system part of this study by Pakistan

Science Foundation (PSF) project No. PSF/Res/C-PIEAS/Phys (218). The MTT assay was funded by the Pakistan Science Foundation (PSF) under project number 733. This research was partly funded by Khalifa University of Science and Technology Competitive Internal Research Award CIRA-ADEK and by Abu Dhabi Award for Research Excellence (AARE) 2019.

Author contributions

A.A., conceptualization, conducted all the experiments, data curation, and writing-original draft. B.A., writing—review &editing, supervision, data curation. S.B., conceptualization, Writing—Review & Editing, microfluidic experimentations, visualization, supervision. S.R., M.B., and T.G., writing—review & editing, visualization. A.G., and R.K. assistance in biological applications. A.U.S., providing SEM analysis. A.A.S. Funding acquisition and writing—review &editing. All authors reviewed the manuscript.

Competing interests

The authors declare no competing interests.

Additional information

Correspondence and requests for materials should be addressed to B.A. or S.B.

Reprints and permissions information is available at www.nature.com/reprints.

Publisher's note Springer Nature remains neutral with regard to jurisdictional claims in published maps and institutional affiliations.